

THE PRODUCTION OF MICRO-DROPLETS BY THE IMPACT OF A DROP ON A HYDROPHOBIC MICRO-GRID

Philippe Brunet¹, Farzam Zoueshtiagh, Alain Merlen

Laboratoire de Mécanique de Lille (LML) UMR CNRS 8107 Cité Scientifique Boulevard Langevin 59655
Villeneuve d'Ascq, France

philippe.brunet@univ-lille1.fr, farzam.zoueshtiagh@univ-lille1.fr, alain.merlen@univ-lille1.fr

Florian Lapierre, Vincent Thomy

Institut d'Electronique de Microélectronique et de Nanotechnologie (IEMN) - UMR CNRS 8520, Cité Scientifique, Avenue Poincaré, BP. 60069, 59652 Villeneuve d'Ascq, France
Florian.Lapierre@etudiant.univ-lille1.fr, vincent.thomy@iemn.univ-lille1.fr

KEY WORDS

Drop production, super-hydrophobicity, free-surface flows

ABSTRACT

We report on experiments of drop impacting a hydrophobic micro-grid, of typical spacing 50 μ m. We find a threshold in impact speed above which a small amount of liquid protrudes the grid and emerges to the other side. For small grid spacings, the emerging liquid takes the form of micro-droplets which size is about the size of the grid step. We propose a method to produce either a mono-disperse spray or a single tiny droplet of sub-nanoliter volume.

LIST OF PARAMETERS

- ρ : liquid density
- σ : surface tension between liquid and surrounding vapour
- η : liquid dynamic viscosity
- d : averaged diameter of the grid hole
- d_{min} and d_{max} : minimum and maximum diameter of the hole
- t : grid thickness
- D : impacting drop diameter
- U_0 : impacting drop speed
- d_s : emerging drop diameter
- U_e : emerging drop speed
- S_i and S_e : hole inlet and outlet sections

1. INTRODUCTION

For discrete micro-fluidics, it is often desired to produce smaller and smaller quantities of liquid in a controlled fashion. Usual methods can be the generation of secondary droplets by drop impact [1, 2], the breakup-up of shear-flow-mediated ligaments [3], the appliance of intense electric fields to conductive liquids [4, 5] or a high-frequency sound wave generated by a piezoelectric acting at the outlet of a nozzle [6].

¹ Corresponding author

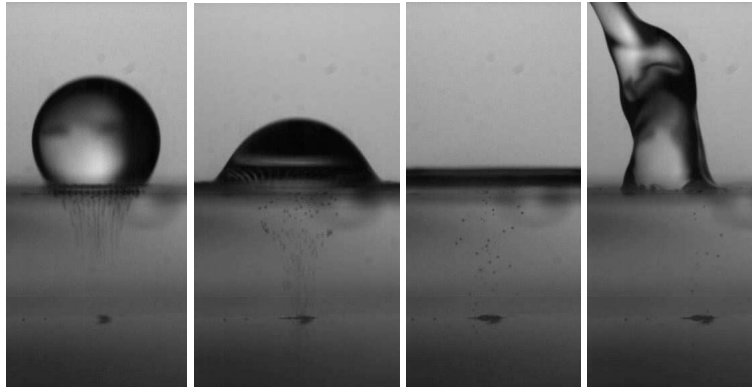


Figure 1: Successive shots showing the impact of a water drop on a hydrophobic grid ($U = 1.54$ m/s, $d_{min} = 20$ μ m). A 'rain' of droplets is observed below the grid.

Here, we propose an alternative method: the impact of drops on a hydrophobic grid of micro-sized holes (diameter d). Figure 2 shows a sequence of such an impact: a few tens of microseconds after the drop has impacted the grid, some liquid previously lying at the base of the drop has been grated over and turned into small - quite monodisperse - droplets. Here we report our first experimental results using hydrophobic grids of different size. We show that, despite the violent character of impact leading to complex flows, the protruded volume depends on the impact speed in a quite reproducible way.

Understanding the basic mechanisms of how the liquid passes through, or is retained by, the grid has multiple applications in processes such as aerosols or filters. More generally, this simple geometry helps to understand how liquid can be captured by surface tension forces, during its contact on a solid of complex shape.

Previous studies on the impact of drops onto holes have been carried out by Lorenceau and co-workers [7]. They used single-hole sieve of size ranging from 100 μ m to 1.7 mm, hence smaller than the capillary length $l_c = \sqrt{\frac{\sigma}{\rho g}}$, and without any non-wetting chemical treatment. The authors proposed and checked that the liquid inertia during impact needs to overcome the capillary forces, in order for some liquid to protrude the hole. This condition is similar to that which selects the size of a drop at the outlet of a tap: a drop falls when its volume is large enough for the weight to overcome capillary retention at the outlet. Here, gravity is replaced by the effective deceleration a of the drop at impact, namely $a \sim U_0^2/D$, where D is the diameter of the impacting drop and U the drop speed at impact. Hence, the condition evidenced in [7] - for the high Reynolds number regime - reads: $l_c^* \leq d$, where l_c^* denotes the effective capillary length built on the drop deceleration at impact $l_c^* = \sqrt{\frac{\sigma D}{\rho U_0^2}}$.

Hence, the natural control parameter of the experiment is the Weber (We) number: $We = \frac{\rho U^2 d}{\sigma}$. Due to the low-viscosity liquid we used (water), the Reynolds number is about 100 or higher. Hence, as shown in [7], retention forces that oppose protrusion are mostly due to capillarity.

Another dimensionless parameter is the Weber number built on the impacting drop diameter instead of the grid spacing: $We_0 = \frac{\rho U_0^2 D}{\sigma}$. This number quantifies the potentiality of the drop to spread horizontally under the action of inertia, independently from its ability to protrude the grid.

2. EXPERIMENTAL SETUP - QUALITATIVE OBSERVATIONS

We use a dripping faucet that releases a drop of pure water (viscosity $\nu = 1$ cSt, surface tension $\sigma = 0.072$ N/m and density $\rho = 1$ g/cm³) from a submillimetric nozzle. In this setup, the diameter of the impacting drop D is determined by the capillary length, and is well reproducible at $D = 2.12 \pm 0.05$ mm. The height of fall h prescribes the velocity at impact: $U_0 = (2gh)^{1/2}$, which can be up to 5.5 m/s. Using backlighting together with a high-speed camera (at a rate of 5000 frames/s, with a resolution of 576 \times 576 pixels or at a rate of 18000 frames/s with 200 \times 200 pixels), the shape of the interface during the spreading and bouncing processes can be

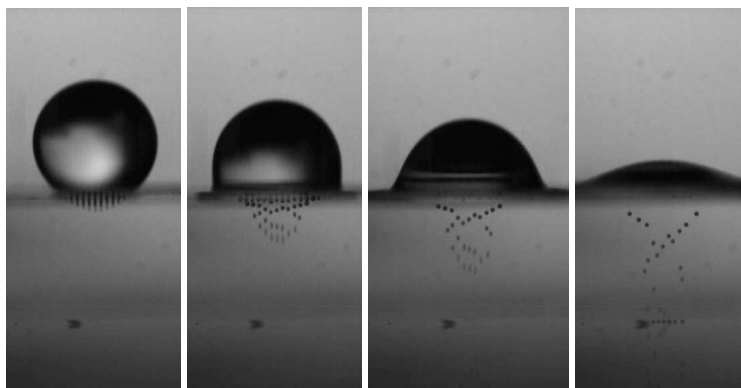


Figure 2: Successive shots showing the impact of a water drop on a hydrophobic grid ($U = 1.44$ m/s, $d_{min} = 43$ μ m). A 'rain' of droplets, slightly larger than the previous case of Fig. 1, is observed below the grid.

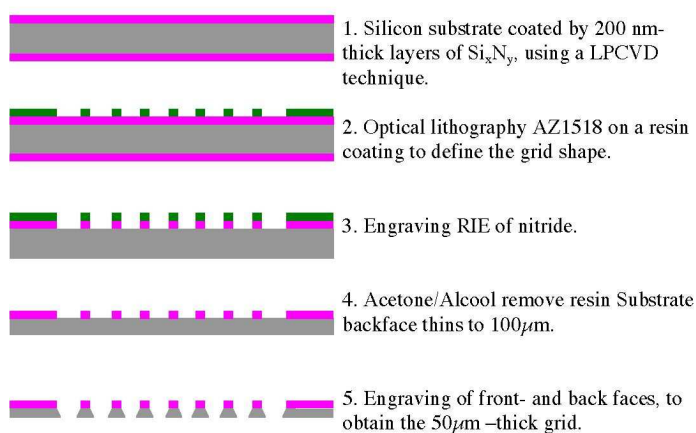


Figure 3: Description of the engraving process that fabricate the micro-grids.

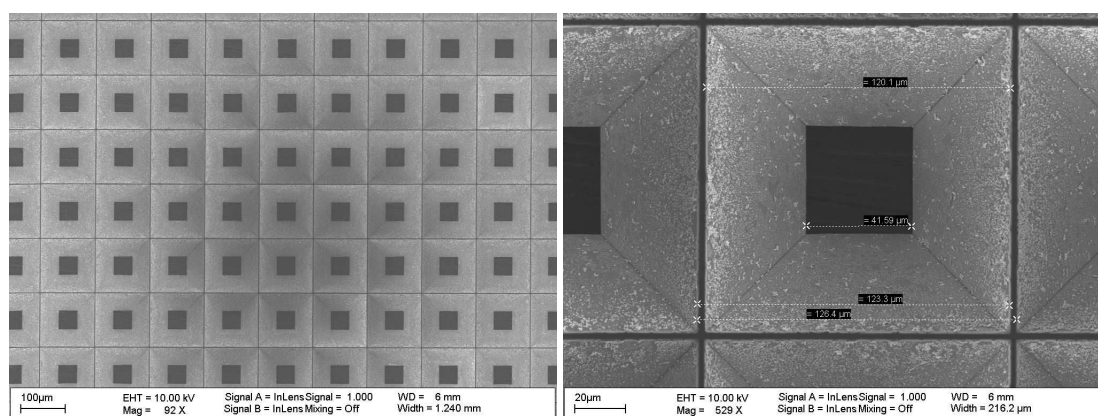


Figure 4: SEM picture of a hydrophobic grid. The trapezoidal holes have d_{min} and d_{max} respectively as smaller and larger width.

determined. The magnification allows for an accuracy of about 15 μ m per pixel.

The grids were fabricated in a clean room using the following process, depicted in Fig. 3: a 200 nm layer of silicium nitride Si_xN_y , deposited with a low-pressure chemical vapor deposition (LPVCD) technique, coats both sides of a 380 μ m silicon substrate $\langle 100 \rangle$ oriented. A mask made of AZ1518 resin is used to engrave Si_xN_y by optical lithography. An engraving process creates grooves at locations where there is no resin, and removes the back face nitride layer. The substrate is then rinsed with acetone and ethanol, and the resin is

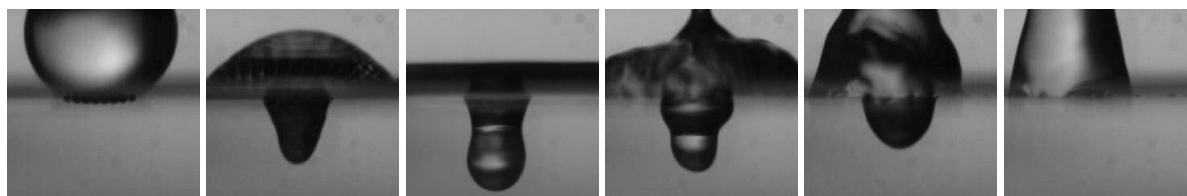


Figure 5: Successive shots showing the impact of a water drop on a hydrophobic grid ($d_{min} = 69 \mu\text{m}$). Although some liquid protruded the grid, it eventually entirely retracts above the grid.

removed. The back side of the substrate, kept in a potassium hydroxide bath during 5+1/2 hours, is etched to a 100 m layer substrate. Then, the whole substrate is thinned to 50 m in the same bath. The trapezoidal shape is obtained due to an anisotropic etching following the $\langle 111 \rangle$ oriented plan. Finally, a hydrophobic coating on the overall surface of the grid is achieved using C_4F_8 plasma deposition (Passivation Gaz: C_4F_8 (50 sccm), passivation time: 10 sec.). A typical resulting grid is shown in Fig. 4. Due to the fabrication process, the holes have a trapezoidal shape, so that d , the length scale on which the Weber number is built, is comprised between d_{min} and d_{max} . The size of grids are summarised in table 1.

Grid number	Thickness t (μm)	d_{min} (μm)	d_{max} (μm)
Grid 1	56	44	125
Grid 2	55	20	100
Grid 5	35	69	120
Grid 6	35	43	94

Table 1: Dimensions of the different grids used.

For small-sized grids (d_{min} less than about $60 \mu\text{m}$), the liquid emerges down the grid in the form of a spray of quite monodisperse droplets as shown in Fig. 2. For the grid with the largest holes (grid 5, $d_{min} = 69 \mu\text{m}$), the liquid emerges as a jet - of diameter much larger than the size of holes - which subsequently either breaks up into a few droplets or retracts entirely towards the upper side of the grid (like in Fig. 5).

3. RESULTS

Quantitatively, we are mostly interested in the situation of the monodisperse spray. The plots in Fig. 7-(a,b) is the number of emerging droplets of liquid detaching down the grid, for 3 different grids, versus (a) the Weber number We and (b) the Weber number built on the impacting drop diameter We_0 . Careful observations, like the sequence of Fig. 2 reveal that the detached droplets are all about the same size, hence constituting a monodisperse spray. Their size is strongly related to the lower size of the holes d_{min} , hence the tiniest observed droplets are about $30 \mu\text{m}$ in diameter, which gives a volume of about 0.01 nanoliter.

The plots reveal two essential features:

- (1) The thresholds for liquid detachment down the grid in We_0 obtained for different grids, range between 40 and 55. But in terms of We , their relative difference is much more pronounced: they lie between 0.4 and 1. A value of 3.9 for We at threshold was measured in [7] for high Reynolds number, and for a hydrophilic single hole (no dependance on the size of the hole was noticed). Although a better wettability would intuitively be a factor that would decrease the threshold, the case of a single hole is different from the case of an ensemble of holes that constitutes the grid. This difference lies also in the dependance of the threshold with the hole diameter, which is observed for the grids but not for a single hole. We give more details in the next theoretical section.

- (2) The number of emerging droplets (or the volume of liquid) increases quite linearly with We or We_0 . Despite the singular dynamics generally observed at impact [1, 2], and the associated non-linear mechanisms that could lead to irregular behavior, the number of droplets (or volume) is quite reproducible. The sequence of Fig. 6 is particularly striking and reveals this reproducibility: it shows a single droplet emerging from the lower

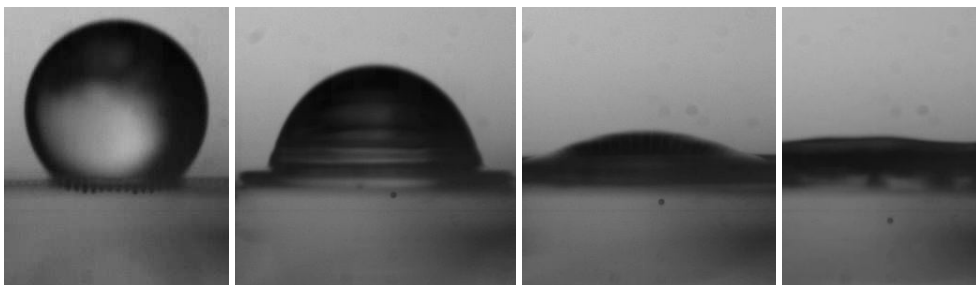


Figure 6: A sequence at threshold: a single tiny droplet emerges down the grid. $U = 1.22$ m/s, ($d_{min} = 43 \mu\text{m}$).

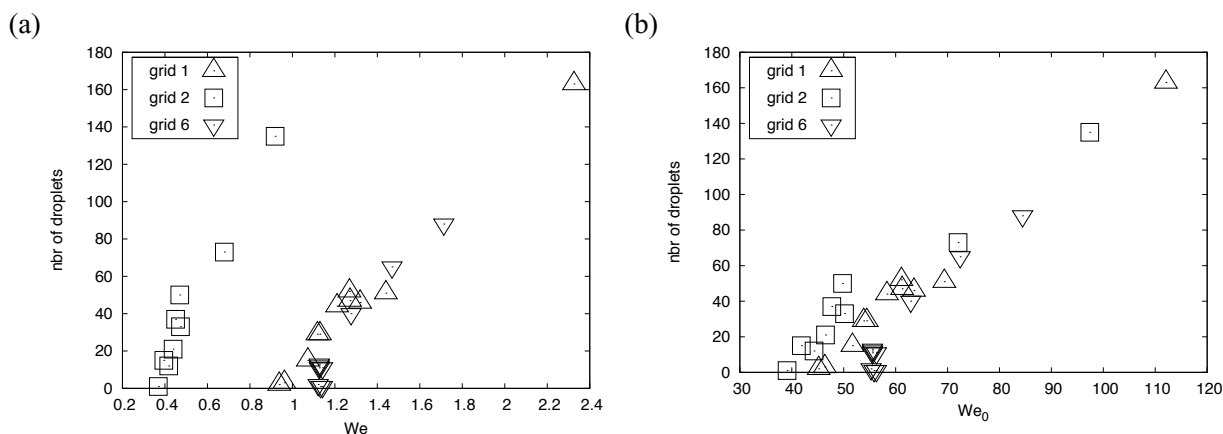


Figure 7: Number of droplets emerging and falling down the grid (a) versus the Weber number We built on the grid hole diameter d_{min} . (b) versus the Weber number built on the impacting drop diameter We_0 .

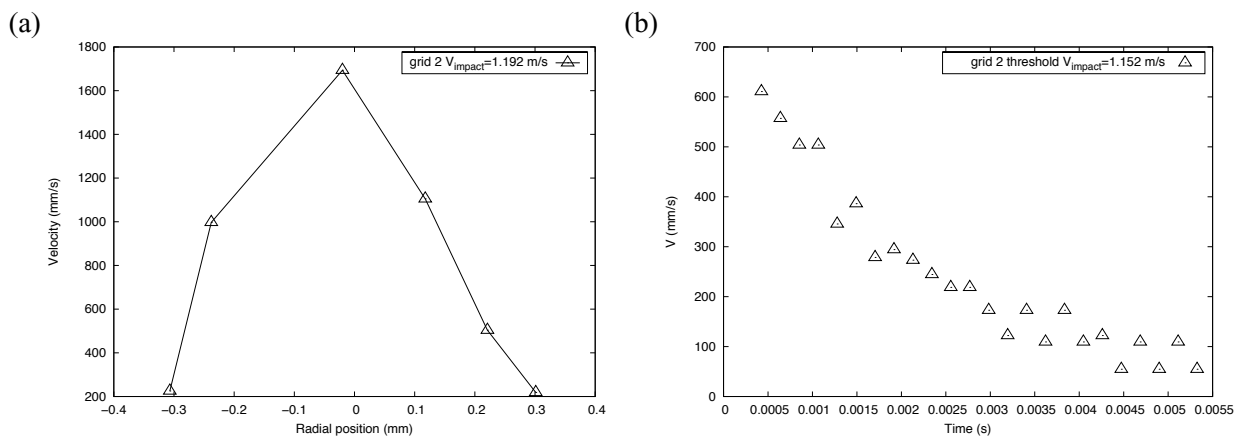


Figure 8: (a) Emerging droplet velocity vs. radial position down the grid (grid 2). $U_0 = 1.192$ m/s. (b) Example of a droplet vertical velocity down the grid, versus time, which clearly show that droplets are slowed down by air friction until they reach a limit speed (grid 2). $U_0 = 1.152$ m/s.

side of the grid after impact. With various tries having the same threshold velocity at impact, one observed each time a single emerging droplet.

We tried to access in more details the behavior of the detaching droplets: it is clearly visible in the sequences of Figs. 1 and 2 that the droplets detaches faster near the apex of impact. Hence, the droplets emerging at the center will hit the ground first. This is confirmed by the direct measurement of the velocity of the droplets just after their emergence, see Fig. 8-a. Not only the droplet speed is maximal at the center, but droplets emerge only in a restricted area around the center. The larger the speed, the larger the zone of emergence. At threshold, of course, a droplet emerges only at the center, with a small speed. Figure 8-b shows the evolution of a droplet velocity after it has detached from the grid (the droplet diameter is about $70 \mu\text{m}$). Despite the droplet is subjected to gravity, it decelerates due to the friction with the ambient air. In fact, in this particular case the droplet initial

speed is about 0.6 m/s, hence much larger than the limit speed governed by the balance between gravity and viscous drag. For a liquid sphere of density ρ_s and diameter d_s , falling in a fluid of viscosity η_f and of density ρ_f , the limit speed is equal to:

$$U_{lim} = \frac{1}{18} \frac{\rho_s - \rho_f}{\eta_f} d_s^2 g \quad (1)$$

The droplet diameter is here $d_s = 45 \mu\text{m}$ (it emerged from grid 2), which gives a limit speed of 0.055 m/s. This value is consistent with the value towards which the speed converges in Fig. 8-b, confirming the visco-gravity equilibrium assumption.

4. THEORETICAL MATTERS

This analysis concerns the prediction of the threshold value. Let call V_0 the volume of fluid initially in the impacting drop and filling the cavity V' or the emitted droplet V . Obviously, $V_0 = V + V'$. At the threshold, the energy balance between the impact and the emission of the droplet can be written:

$$\frac{1}{2} \rho V U_e^2 + \pi d_s^2 \sigma + \sigma S_o - \frac{1}{2} \rho V_0 U_0^2 - \sigma S_i = T \quad (2)$$

where U_0 and U_e are respectively the impact velocity and the velocity of the emitted droplet. Sections S_i and S_o are the the inlet and outlet sections of the hole (they are not equal as the holes are trapezoidal), ρ the density of the liquid and T the work of the external forces on the fluid volume during the process. These forces represent essentially the pressure due to the impact inside the impacting drop which pushes the liquid through the hole like a syringe, and the surface tension and the triple line forces which resist to this motion like a membrane. The hydrophobicity of the surfaces is taken into account by counting the capillary energy as positive (hence taking the contact angle equal to 180°). When T is positive, the "syringe effect" is predominant, when it is negative the fluid crosses the grid by inertia but the "membrane effect" slows the emerging droplet down. Of course in present analysis the viscous dissipation is neglected as suggested by Lorenceau et al. [7] for high Reynolds numbers. In dimensionless form, the previous balance gives:

$$\frac{U_e^2}{U_0^2} + \frac{3/2}{\text{We}} \left(1 + \frac{S_o - S_i}{\pi d_s^2} \right) - \left(1 + \frac{V'}{V} \right) = \frac{T}{\frac{1}{2} \rho U_0^2 V} \quad (3)$$

where the Weber number is built with d_s the diameter of the emitted droplet $W_{ed} = \frac{\rho U_e^2 d_s}{\sigma}$, and by taking $V = \frac{4\pi}{3} d_s^3$. The diameter d_s is comprised between d_{min} and d_{max} , independently of the impact speed. The work T depends on the geometry of the grid and can be positive or negative at the threshold according to the balance between the impact pressure forces and the surface tension effects.

For the case treated by Lorenceau where $S_i = S_o$, the previous formula gives a Weber number of 3.9 considering $T \approx 0$ due to the fact that the grid is very thin, compared to the emitted droplet. This value is consistent with the experimental value of approximately 3.5 found by Lorenceau et al. but with a We based on the hole diameter smaller than the one of the emitted droplet. For the present experiments¹, grid 2 gives a negative value of about $\frac{T}{\frac{1}{2} \rho V_i^2 V} \approx -8$ which supposes that the surface tension resists the protrusion because of the high contraction effect and the relatively high ratio $\frac{V'}{V} \approx 3.5$. Most of the pressure work is utilised to fill the cavity and not to emit a droplet. For grid 6 for which $\frac{V'}{V} \approx 0.33$ the work is positive, showing that the pressure inside the impacting drop pushes the fluid through the hole $\frac{T}{\frac{1}{2} \rho V_i^2 V} \approx 4$. These values underline the fact that the grid design is a very sensitive parameter and that the process is extremely geometry dependent.

If we wish to give a physical meaning for the quantity T , let us remind the following: when a drop impacts a solid (or a thin liquid layer), a pressure singularity develops at the location of impact (see [1] and references therein). This is due to the very brief transfer of momentum from the vertical (up-down) direction to the horizontal (outwards) direction. With a plain solid, the mass of liquid cannot penetrate in and hence the liquid flow inside the impacting drop changes its direction at the location of impact, in a very brief amount of time, creating the pressure singularity. But if the solid is porous like our grid, some liquid is allowed to pass through and some

¹ The quantity V'/V is determined by taking a square-base pyramidal shape for the holes, and U_e is taken very small compared to U_0 .

liquid is stopped by the solid. In the vicinity of each solid part of the grid, a similar pressure peak is generated, which leads to an overall (and broader) pressure peak around the location of impact. The pressure field that built up in that way probably contributes to the liquid protrusion, which is reflected by a positive value for T , the external forces. It is possibly one of the causes why our experiments show a threshold Weber number between 0.4 and 1, whereas Lorenceau et al. [7] found a Weber number at around 3.5^2 . The geometry of the grid is more susceptible to induce a built up pressure on top of the substrate than the geometry of a single hole. Another possible cause for the discrepancy between our thresholds and Lorenceau's measurements is that our holes are trapezoidal shaped, whereas Lorenceau's are straight. The choice for the length scale d in We is a bit puzzling, as d ranges between d_{min} and d_{max} . In Figs. 7, we arbitrarily took $d = d_{min}$, but the emerging droplets diameter d_s chosen, is larger. The analysis of eqs. (2) and (3) lets d_s appear as a natural choice, although this length is not a control parameter. In short, these relationships help to predict the value of T and threshold Weber number, from the grid geometry and the measurements of the velocities of impacting drop and emerging droplets.

5. CONCLUSIONS

In summary, our drop impact experiments using hydrophobic micro-grids as substrate show an original and reproducible way to generate tiny droplets of sub-nanoliter volume. For grids of spacing less than about $60 \mu\text{m}$, we evidenced that some liquid protrudes the grid and emerges down its bottom side under the form of small droplets, providing that the speed at impact is large enough. The droplets are about the same diameter as the grid spacing, and their size is well monodisperse. Within the accuracy allowed by our visualisations (1 pixel is about 8 microns), it was not possible to distinguish any difference in the droplet size, i.e. their diameter was always measured with the same number of pixels.

Future studies could explore similar experiments with grids of much larger thickness. Thick hydrophobic grids could constitute low-friction substrates for droplet handling in lab-on-chip experiments. Recent drop impact experiments [10, 11] on microtextured surfaces showed that the height of the texture was crucial to delay the undesired transition from Cassie-Baxter [8] to Wenzel [9] states, occurring when liquid is impaled through the texture. A grid constitutes a bottomless substrate, which could be an asset for generating a reverted Wenzel-to-Cassie transition with the help of a pressure source below the substrate, something which is not possible with the usual arrays of micro-pillars.

ACKNOWLEDGEMENTS

REFERENCES AND CITATIONS

- [1] A.L. Yarin, *Drop impact dynamics: Splashing, spreading, receding, bouncing ...*, Annu. Rev. Fluid Mech. **38**, 159-192 (2006).
- [2] R.D. Deegan, P. Brunet and J. Eggers, *Complexities of splashing*, Nonlinearity **21**, C11-C11 (2008).
- [3] P. Marmottant and E. Villermaux, *On spray formation*, J. Fluid Mech. **498**, 73-112 (2004).
- [4] A.M. Gaan Calvo, *Enhanced Liquid Atomization: From Flow-Focusing to Flow-Blurring*, Appl. Phys. Lett. **86**, (2005).
- [5] R.T. Collins, J.J. Jones, M.T. Harris and O.A. Basaran, *Electrodynamic tip streaming and emission of charged drops from liquid cones*, Nat. Physics **4** 149-154 (2008).
- [6] J.M. Scheider and C.D. Hendricks, *Source of uniform-sized liquid droplets*, Rev. Sci. Instrum. **35** 1349-1350 (1964).
- [7] E. Lorenceau and D. Quéré, *Drops impacting a sieve*, J. Coll. Interf. Sci. **263** 244-249 (2003).
- [8] A. Cassie and S. Baxter, *Trans. Faraday Soc.* **40**, 546 (1944).
- [9] R. Wenzel, *Ind. Eng. Chem.* **28**, 988 (1936).
- [10] D. Bartolo et al., *Europhys. Lett.* **74** 299 (2006).
- [11] M. Reyssat et al., *Europhys. Lett.* **74** 306 (2006).

² A value based on the radius of the hole instead of the diameter, which means that the discrepancy is even larger.